Machine Vision for Astronomical Images Using the Canny Edge Detector

Sergii Khlamov [1], Iryna Tabakova [1], Tetiana Trunova [1] and Zhanna Deineko [1]

[1] *Kharkiv National University of Radio Electronics, Nauki avenue 14, Kharkiv, 61000, Ukraine*

Abstract

In this paper we have presented a realization of the machine vision purposes in scope of the processing of astronomical frames by the Canny edge detector. Its main purpose is to select image's borders of object with the unknown shape in the frame's background using the different known recognition patterns. Parameters for the Canny edge detector are determined automatically by the results of frame pre-processing and are unique for each image in the input data set. The Canny edge detector was realized as a tool using the C++ programming language. Implementation of the machine vision purposes was tested using the astronomical frames with different patterns, object shapes, sizes, and resolutions.

Keywords

Machine vision, image recognition, image processing, Canny edge detector, object detection, recognition patterns

1. Introduction

The astronomical frames in the common case are made by the charge-coupled devices (CCD) [1] and can be received from the different sources: archives, servers, predefined series or "live" (online) data streams. There are also various machine vision purposes [2] that include analyzing, understanding digital images, methods for acquiring, processing and extraction of high-dimensional information to produce symbolic or numerical data in form as decisions [3].

The machine vision and data mining [4] purposes regarding the astronomical frame processing are related to the following features: filtering [5], brightness equalization with background alignment [6], images detection of objects [7], motion detection of objects [8], astrometry (estimation of the object's position in an image, which can be converted to position in the sky) [9], photometry (estimation of the object's brightness) [10], determination of the object's parameters and its visible motion [11], reference objects cataloging [12], objects recognition [13, 14], Wavelet coherence analysis [15], etc. There are several mathematical filters that are different by their nature but can be used at the pre-processing stage in the pipeline for CCD-images [16] before the general frame processing method:

- **fast Fourier transform** (FFT), as an algorithm, which computes the discrete Fourier transform (DFT) of a sequence, or its inverse (IDFT) [17].
- **low-pass filter** [18] – data cleaning process for bypassing the different artifacts of the instrumental measurements. Such a filtering algorithm also attenuates signals with frequencies higher than the cutoff frequency and passes only the signals with a frequency lower than a selected cutoff frequency.
- **edge detection** methods [19] that are aimed at the edges identifying like curves in a frame, at which the image brightness changes sharply or has discontinuities.
- **corner detection** methods [20] that are used in the machine vision process to get the appropriate kinds of the features of an image.

Information Technology and Implementation (IT&I-2022), November 30 - December 02, 2022, Kyiv, Ukraine
EMAIL: sergii.khlamov@gmail.com (S. Khlamov); iryna.tabakova@nure.ua (I. Tabakova); tetiana.trunova@nure.ua (T. Trunova); zhanna.deineko@nure.ua (Zh. Deineko)
ORCID: 0000-0001-9434-1081 (S. Khlamov); 0000-0001-6629-4927 (I. Tabakova); 0000-0003-2689-2679 (T. Trunova); 0000-0003-0175-4181 (Zh. Deineko)

- **blob (point) detection** methods [21] that are aimed for the identifying process of the various regions of the investigated objects in the astronomical CCD images. Such regions have differences in color and brightness/gray shade, which are comparable with the adjacent regions. The blob is a kind of region with points or even pixels that have the same constant or approximately constant properties, so all such points or even pixels in the blob are the same.
- **ridge detection** methods [22] that are aimed at the ridge's localization in the frame that defined as curves where its points are the local maximums of the image function, like the geographical ridges.

The object's recognition process using the predefined recognition pattern can be simplified by the preparing more accurate determined image's borders of object [23]. There are a lot of different patterns or types of objects in an image: point, long, blurred and objects with flare or intersection with another objects. Some of them are galaxies, stars, robots, drones [24], rockets, satellites [25], and even small Solar System objects [26].

So, for our research we selected the Canny edge detector from the edge detectors family [19] to analyze its ability to identify edges of the different astronomical objects in images, which have more complicated structure and random background noise.

In this paper we presented the several mostly known recognition patterns for the astronomical frames, which are commonly used during the astronomical image processing like classification. Also, we presented the real examples of applying the Canny edge detector implemented into the developed tool using the C++ programming language. This tool is a realization of the machine vision purposes for processing of the astronomical frames with different patterns, sizes, object shapes and resolutions.

2. Astronomical object classification

One of the main directions for the image processing in astronomy is the object classification. This process is also related to the one step from the general (KDD) process [27].

There are two known helpful concepts in the astronomical object classification. They are completeness (also known as recall) and efficiency (also known as precision). The completeness concept is defined in terms of the true positive (TP) and false positive (FP). The efficiency concept is defined in terms of the true negative (TN) and false negative (FN).

The completeness concept is the number of objects that are really related to the appropriate class with some pattern, as mentioned in the following formula [7, 14]:

$$completeness = \frac{TP}{TP + TN} \tag{1}$$

The efficiency concept is the number of objects that were already classified and really related to the appropriate pattern, as mentioned in the following formula [8, 14]:

$$efficiency = \frac{TP}{TP + FP} \tag{2}$$

Such two metrics are very interesting for the astrophysics research in case when completeness and efficiency are the highest. The importance of each quantity is often depended on the situation. For example, an investigation of the rare objects that generally requires a high completeness while allows the lower efficiency, but the statistical clustering or classification of cosmological and astrophysical objects requires the high efficiency, even if the completeness of such procedure is very expensive.

The astronomical object classifications can be also performed by the bivariate luminosity function and the morphology-density relation where both a digital sky survey of this size and detailed Hubble types are used. Such realization uses a committee of Artificial Neural Networks (ANNs) [28] in the "waterfall" arrangement, in which the output from one ANN is the input of other ANN. This detalization produces the more detailed classes and subclasses, that improves their results using the spectral principal components and investigation of their kinematics.

The different genetic algorithms with evolving the ANNs are used for the attribute selection and classification of the "bent-double" galaxies in the FIRST (Faint Images of the Radio Sky at Twenty-cm) [29] radio survey data. FIRST is the project, which was developed for the generating a radio equivalent of the Palomar Observatory Sky Survey over 10 thousand degrees^2 of the North and South Galactic Caps.

Using the NRAO Very Large Array (VLA) and an automated mapping pipeline, the FIRST project produced images with the following characteristics: 1.8" pixels, typical root mean square (RMS) of 0.15 mJy, image resolution of 5". The detection threshold was used at the 1 mJy source, and there were about 90 sources per degree^2, where about 35 percent of which have the formed structure with scales from 2-30". And only 30 percent of the FIRST sources have analogues in the known modern Sloan Digital Sky Survey (SDSS) catalogue [30].

So, the radio morphology includes the compact nucleus of the radio galaxy and extremely long jets. Thus, in this way the bent-double morphology detects the galaxy cluster presence. Such morphology can be performed by the different approaches. Some of them are like combination of the ensembles of ANN and the locally weighted regression or even by using the fuzzy algebra and heuristic methods, anticipating the importance of probabilistic studies that are just now beginning to emerge.

3. Recognition patterns

The pattern recognition techniques are the base of the machine vision purposes into processing of the astronomical frames. Such recognition techniques are related to the astronomical object classification and simplify this process using the especial methods, templates, patterns, etc. These algorithms are used for the assignment of the initial input data to a certain class or group by selecting of the major features, which characterize this group [31]. So, for the objects in images received as real sets of astronomical frames, the following different recognition patterns can be applied [32].

3.1. Point objects

The point objects in the astronomical frame have a round shape. These objects have only one brightness peak in its center. Such example of the point objects in the astronomical frame is presented in the Figure 1.

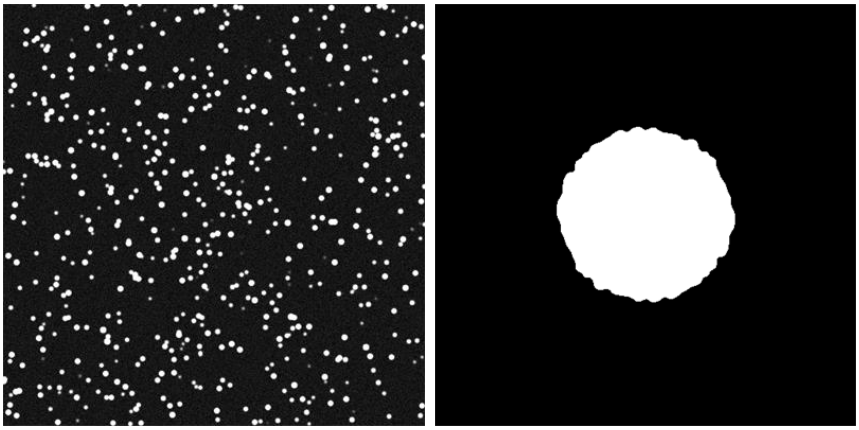

Figure 1: Astronomical image with the point objects: spatial domain (left) and its frequency domain (right)

3.2. Long objects

The extended or long objects in the astronomical frame have the round shape at the end of their form and at least 1:4 or even more semi-axes ratio. These objects have several brightness peaks that

very closely lie along the line in the direction of object. Such example of the long objects in the astronomical frame is presented in the Figure 2.

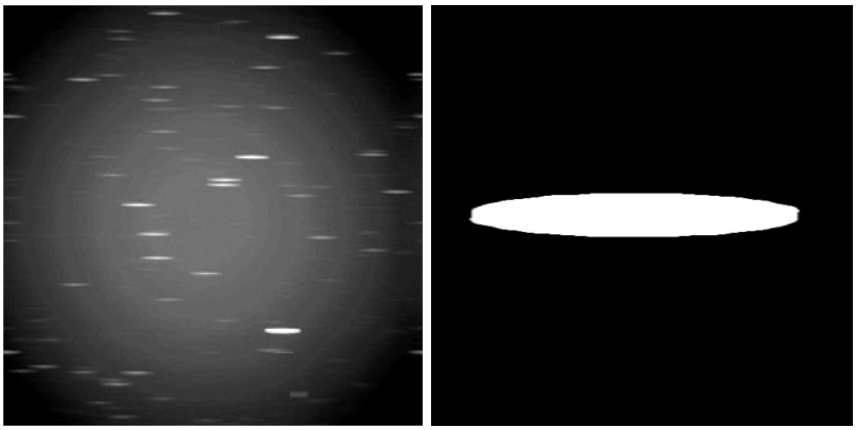

Figure 2: Astronomical image with the long objects: spatial domain (left) and its frequency domain (right)

3.3. Blurred objects

The blurred objects in the astronomical frame have the round shape at the end of their form and up to 1:4 semi-axes ratio. These objects have the same properties with extended/ long objects but have the different origin nature. The reasons of such frame's creation are the following: various telescope's aberrations, different fails in the diurnal tracking, telescope coma [33], etc. Such example of the blurred objects in the astronomical frame is presented in the Figure 3.

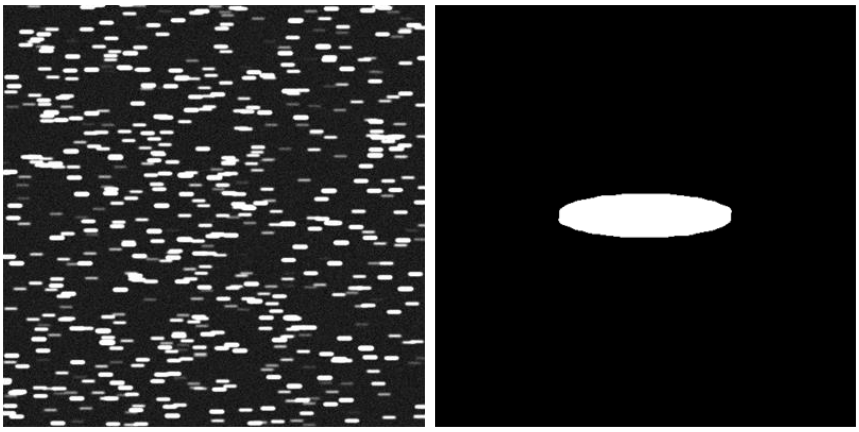

Figure 3: Astronomical image with the blurred objects: spatial domain (left) and its frequency domain (right)

3.4. Objects with flare or intersection with other objects

This type of the object's recognition pattern is not so general, but also can be as a combination of other patterns, e.g., point, long and blurred objects. The major singularity of it is the crossing with other objects in the astronomical frame where the brightness of the closely located object is more than brightness of the investigated object.

Another case of appearance of such superfluous flare is the very long exposure time. This situation is very complicated for the automated machine vision because the brightness peak of such intersected objects are mixed and unspecified.

Such example of the objects with flare and intersection with another objects in the astronomical frame is presented in the Figure 4.

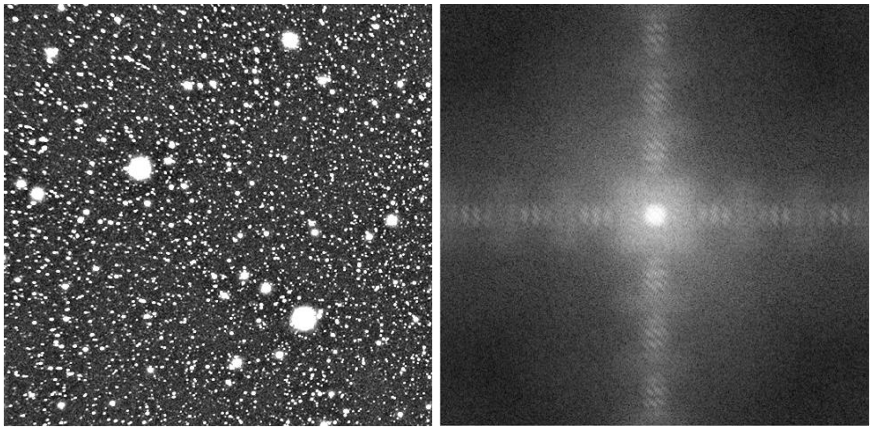

Figure 4: Astronomical image with the objects with flare and intersection with another objects: spatial domain (left) and its frequency domain (right)

4. Canny edge detector

The Canny edge detector is an operator from the edge detection family, which uses a multi-steps algorithm to detect the wide range of edges or corners in the CCD-images. The Canny edge detection is a method, which helps to extract the useful structure information of the various vision objects and reduce the amount of data for the further processing. Such filter is widely used in the different computer vision systems.

The developer Canny has found that the requirements for the edge detection application on diverse vision systems are comparatively similar. In this case, the edge detection technique can be used in a very wide range of conditions [34].

4.1. Criteria

There are several common criteria for the edge detection:

- Detection of edges with the lower rate of error – the detection should precisely catch as many edges presented in the CCD-image as possible.
- The edge point, which was detected from the operator will accurately localize in a center of the CCD-image's edge or corner.
- A given edge in the CCD-image will be marked only one time, and where possible, image noise will not create false edges or corners.

4.2. Processing steps

The processing algorithm of the Canny edge detector consists of the following five processing steps [35]:

- Applying of the Gaussian filter [18] to remove the noise by smoothing the CCD-image under processing using the following equation:

$$H_{ij} = \frac{1}{2\pi\sigma^2} exp\left(-\frac{\left(i-(k+1)\right)^2 + \left(j-(k+1)\right)^2}{2\pi\sigma^2}\right), \quad (3)$$

  where $1 \leq i, j \leq (2k+1)$.
- Determining of the image's intensity gradients using the following equation:

$$G = \sqrt{G_x^2 + G_y^2}, \tag{4}$$

$$G_x = \begin{bmatrix} -1 & 0 & +1 \\ -2 & 0 & +2 \\ -1 & 0 & +1 \end{bmatrix} * A; \quad G_y = \begin{bmatrix} -1 & -2 & -1 \\ 0 & 0 & 0 \\ +1 & +2 & +1 \end{bmatrix} * A \tag{5}$$

where G_x and G_y are two images which at each point contain the horizontal and vertical derivative approximations respectively; A is a source image.

- Applying of thresholds of the gradient magnitude and performing the lower bound cut-off reduction for getting the rid of mock response for the edge detection.
- Applying of the predefined double threshold for determination of the potential edges in the CCD-image under processing.
- Finalizing of the edges detection by reducing all other edges that are not connected to the strong edges and weak.

4.3. Thresholds

For the last processing step of the Canny edge detector, the higher and lower threshold values are selected. If the gradient value of an edge pixel is higher than the higher threshold value, it is marked as a strong edge pixel.

If a gradient value of an edge pixel is lower than the higher threshold value and higher than the lower threshold value, it is marked as a faint edge pixel. If the gradient value of an edge pixel is lower than the lower threshold value, it is rejected.

Such 2 critical values are defined according to the given input astronomical image [36].

5. Image recognition test examples

The Canny edge detector can be used aa a pre-processing method in the pipeline. The proper place for it is before the main algorithm using for the image processing (classification [31] and recognition [5] of objects, parameters estimation of the image or apparent motion of object [11]).

In our research we applied the Canny edge detector after the brightness alignment and background equalization processing using the inverse median filter [6]. We decided this because of the more precise object's edge detection after applying the Canny edge detector without the redundant noises in astronomical frame.

Under the current research we took astronomical frames for the image's recognition purposes with the following various resolutions: 512 x 512, 768 x 512, 3056 x 3056, 4008 x 2672 pixels. Also, the appropriate different conditions were used during the observation. Such astronomical frames were received from the several real observatories and used as the test examples.

These test data were selected in scope of the current research from the following real observatories: ISON-NM [37], ISON-Kislovodsk [37], Vihorlat Observatory in Humenne [10] and Mayaki observing station of "Astronomical Observatory" Research Institute of I. I. Mechnikov Odessa National University [38] with unique observatory codes "H15", "D00", "Humenne" and "583" accordingly.

The information about these observatories is provided in the Table 1. The observatory codes are unique and approved by the Minor Planet Center (MPC) [39] of the International Astronomical Union (IAU) [40].

Image recognition test examples are consisting of the different series of astronomical CCD-frames that were collected during the regular observations by the various CCD-cameras. The information about the CCD-cameras that are installed on the telescopes from the observatories list above is presented in the Table 2.

This table contains the following information about CCD-camera: model and its parameters, like resolution, pixel size and exposure time.

Table 1
Information about observatories

Observatory	Code	Telescope
ISON-Kislovodsk	D00	19.2 cm wide-field GENON (VT-78) telescope
ISON-NM	H15	0.4 m SANTEL-400AN telescope
Vihorlat Observatory	Humenne	Vihorlat National Telescope (VNT) – Kassegren telescope with 1 m main mirror with focal length 8925 mm
Vihorlat Observatory	Humenne	Celestron C11 telescope – Schmidt-Cassegrain telescope with 28 cm main mirror with focal length 3060 mm
Astronomical Observatory	583	0.48 m AZT-3 telescope – reflector with focal length 2025 mm
Observatory	Code	Telescope
ISON-Kislovodsk	D00	19.2 cm wide-field GENON (VT-78) telescope
ISON-NM	H15	0.4 m SANTEL-400AN telescope

Table 2
Information about CCD-cameras

Code	CCD-camera	Resolution	Pixel size	Exposure time
D00	FLI ML09000-65	4008 × 2672 pixels	9 microns	180 seconds
H15	FLI ML09000-65	3056 × 3056 pixels	12 microns	150 seconds
Humenne	FLI PL1001E	512 × 512 pixels	12 microns	150 seconds
Humenne	G2-1600	768 × 512 pixels	9 microns	180 seconds
583	Sony ICX429ALL	795 × 596 pixels	12 microns	150 seconds

Each series of CCD-frames includes the different investigated objects in each frame of series. Processing results of some examples of the astronomical frames according to the different recognition patterns of objects described above using the developed tool with implemented Canny edge detector are presented in the Figure 5.

The processing results and subsequent analysis showed that the Canny edge detector has a good accuracy with edge detection in the astronomical frames, which contain the point objects and the single long objects. The processing results of the edge detection for the blurred objects are not so precise. The reason of this is that there are few brightness peaks are very closely presented along a line of the direction of object. So, images of the several objects are mistakenly merged into the one object, which makes further processing very uncertain and complicated. So, as a result, the Canny edge detector is not so effective for using with such astronomical recognition patterns.

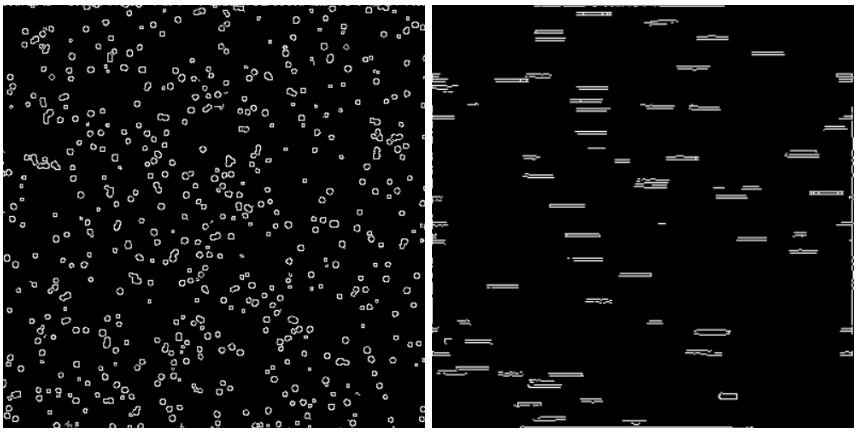

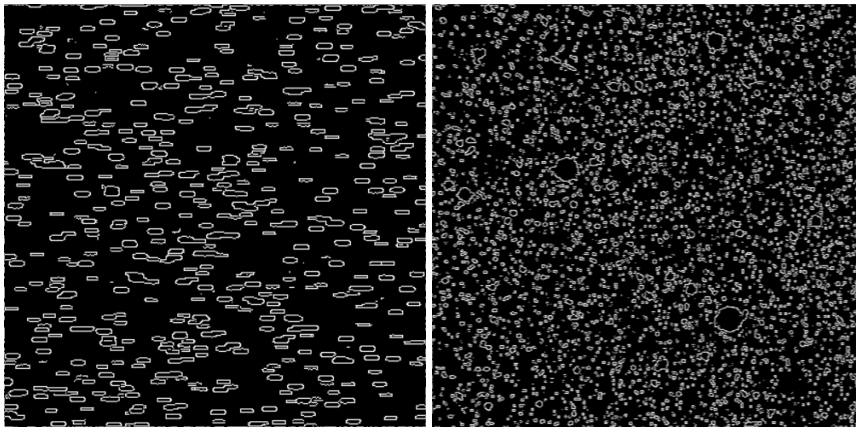

Figure 5: Processing results of astronomical frames with several recognition patterns of point, long, blurred objects and objects with flare

6. Conclusions

The tool with implementation of the machine vision purposes into processing of the astronomical frames using Canny edge detector was developed as research under the CoLiTec project [27]. The tool with a realization of the Canny edge detector uses the C++ programming language, OpenCV mathematical library and QT graphical library. The especial test data in view of sets with astronomical CCD-frames [41] were selected for the current research by the various observatories equipped with the different telescopes. Such astronomical frames had the various observation conditions, resolutions for the required quality and presence of objects in the frames that can be recognized by the predefined investigated patterns. The quality indicators, like conditional probability of true detection and accuracy of the edge detection of objects were analyzed, which made possible to make the resolution.

With help of applying the Canny edge detector under the pre-processing stage in a pipeline for the astronomical frames the precision of the major image processing methods (classification [27] and recognition [5] of objects, matched filtration [42], parameters estimation of the image or apparent motion of object [11], photometry [43]) increases by 5-20%. As results showed, the Canny edge detector applying increases the precision of the edge detection for the point and the single long objects. For the blurred objects in the astronomical frames, it is not so effective because of the difficulty increasing of detection and the chance to lose the object. The received results after processing including the generated experiments will be also used for the machine learning [44] and time series [45] analysis.

7. Acknowledgements

The authors thank all observers, online services, and tools, which provided their data for the current investigation and testing of the developed tool with implementation of the machine vision purposes into processing of the astronomical frames using Canny edge detector.

8. References

[1] G. E. Smith, The invention and early history of the CCD, Rev. Mod. Phys, vol. 3, issue 82, pp. 2307-2312, 2010.
[2] R. Klette, Concise computer vision, Springer, London, 2014.
[3] C. Steger, M. Ulrich, and C. Wiedemann, Machine vision algorithms and applications, John Wiley & Sons, 2018.
[4] S. Cavuoti, M. Brescia, and G. Longo, Data mining and knowledge discovery resources for astronomy in the Web 2.0 age, Proceedings of the SPIE Astronomical Telescopes and

Instrumentation, Software and Cyberinfrastructure for Astronomy II, vol. 8451, 2012. doi: 10.1117/12.925321.
[5] S. Khlamov, et al., Recognition of the astronomical images using the Sobel filter, Proceedings of the International Conference on Systems, Signals, and Image Processing, IWSSIP 2022, 4 p., 2022. doi: 10.1109/IWSSIP55020.2022.9854425.
[6] V. Savanevych, et al., CoLiTecVS software for the automated reduction of photometric observations in CCD-frames, Astronomy and Computing, vol. 40 (100605), 15 p., 2022. doi: 10.1016/j.ascom.2022.100605.
[7] V. Savanevych, et al., Formation of a typical form of an object image in a series of digital frame, Eastern-European Journal of Enterprise Technologies, vol. 6, issue 2 (120), pp. 51–59, 2022. doi: 10.15587/1729-4061.2022.266988.
[8] T. Ando, Bayesian model selection and statistical modeling, CRC Press, 2010.
[9] V. Kudak, V. Klimik, and V. Epishev, Evaluation of disturbances from solar radiation in orbital elements of geosynchronous satellites based on harmonics, Astrophysical Bulletin, vol. 65 (3), pp. 300-310, 2010. doi: 10.1134/S1990341310030120.
[10] K. M. Hampson, D. Gooding, R. Cole, and M. J. Booth, High precision automated alignment procedure for two-mirror telescopes, Applied Optics, vol. 58, pp. 7388-7391, 2019.
[11] A. Massone, A. Perasso, C. Campi, and M. Beltrametti, Profile detection in medical and astronomical images by means of the Hough transform of special classes of curves, Journal of Mathematical Imaging and Vision, vol. 51 (2), pp. 296-310, 2015. doi: 10.1007/s10851-014-0521-4.
[12] V. Savanevych, et al., Selection of the reference stars for astrometric reduction of CCD-frames, Advances in Intelligent Systems and Computing, vol. 1080, pp. 881–895, 2020. doi: 10.1007/978-3-030-33695-0_57.
[13] J. Luan, Book review: Practical algorithms for image analysis: Description, examples, and code, Discrete Dynamics in Nature and Society, vol. 6 (3), pp. 219–220, 2001. doi: 10.1155/s1026022601000243.
[14] R. Gonzalez, and R. Woods, Digital image processing, 4th edition, NY: Pearson, 2018.
[15] M. Dadkhah, et al., Methodology of wavelet analysis in research of dynamics of phishing attacks, International Journal of Advanced Intelligence Paradigms, vol. 12(3-4), pp. 220-238, 2019. doi: 10.1504/IJAIP.2019.098561.
[16] J. R. Janesick, Scientific charge-coupled devices, SPIE press, 2001. doi: 10.1117/3.374903.
[17] S. Haynal, and H. Haynal, Generating and searching families of FFT algorithms, Journal on Satisfiability, Boolean Modeling and Computation, vol. 7(4), pp. 145-187, 2011. doi: 10.48550/arXiv.1103.5740.
[18] J. Karki, Active low-pass filter design, Texas Instruments application report, 2000.
[19] J. M. Park, and Y. L. Murphey, Edge detection in grayscale, color, and range images, Wiley Encyclopedia of Computer Science and Engineering, pp. 1-16, John Wiley & Sons, Inc., 2008. doi: 10.1002/9780470050118.ecse603.
[20] E. Rosten, and T. Drummond, Machine learning for high-speed corner detection, Lecture Notes in Computer Science, vol. 3951, pp. 430-443, 2006.
[21] T. Lindeberg, Scale selection properties of generalized scale-space interest point detectors, Journal of Mathematical Imaging and vision, vol. 46(2), pp. 177-210, 2013. doi: 10.1007/s10851-012-0378-3.
[22] T. Lindeberg, Edge detection and ridge detection with automatic scale-selection, International journal of computer vision, vol. 30(2), pp. 117–156, 1998.
[23] M., Svensén, and C. M. Bishop, Pattern recognition and machine learning, Springer, 2007.
[24] M. Ivanov, et al., Effective informational entropy reduction in multi-robot systems based on real-time TVS, IEEE International Symposium on Industrial Electronics, pp. 1162–1167, 2019. doi: 10.1109/ISIE.2019.8781209.
[25] V. Akhmetov, et al., Cloud computing analysis of Indian ASAT test on March 27, 2019, Proceedings of the 2019 IEEE International Scientific-Practical Conference: Problems of Infocommunications Science and Technology, PIC S and T 2019, pp. 315–318, 2019. doi: 10.1109/PICST47496.2019.9061243.
[26] M. Mahlke, et al., The ssos pipeline: Identification of Solar System objects in astronomical images, Astronomy and Computing, vol. 28, 100289, 2019. doi: 10.1016/j.ascom.2019.100289.

[27] K. Borne, Scientific data mining in astronomy, Data Mining and Knowledge Discovery Series, Chapman and Hall/CRC, pp. 115-138, 2008.
[28] A. A. Collister, O. Lahav, ANNz: Estimating Photometric Redshifts Using Artificial Neural Networks, The Publications of the Astronomical Society of the Pacific, vol. 116, issue 818, pp. 345-351, 2004. doi:10.1086/383254.
[29] N. Thyagarajan, D. J. Helfand, R. L. White, and R. H. Becker, Variable and Transient Radio Sources in the FIRST Survey, The Astrophysical Journal, vol. 742, id 49, 15 p., 2011. doi: 10.1088/0004-637X/742/1/49.
[30] Zhenping Yi, et al., Automatic detection of low surface brightness galaxies from SDSS images, MNRAS, stac775, 2022. doi:10.1093/mnras/stac775.
[31] W. Burger, and M. Burge, Principles of digital image processing: fundamental techniques, New York, NY: Springer, 2009.
[32] W. R. Howard, Pattern recognition and machine learning, Kybernetes, 2007.
[33] D. J. Schroeder, Astronomical optics, Elsevier, 1999.
[34] T. Moeslund, Canny edge detection, Laboratory of Computer Vision and Media Technology, Aalborg University, Denmark, 2009.
[35] H. Scharr, Optimal operators in digital image processing, Doctoral dissertation, Rupertus Carola University, 2000.
[36] R. Kimmel, and A. M. Bruckstein, Regularized Laplacian zero crossings as optimal edge integrators, International Journal of Computer Vision, vol. 53(3), pp. 225-243, 2003. doi: 10.1023/A:1023030907417.
[37] I. Molotov, et al., ISON worldwide scientific optical network, Fifth European Conference on Space Debris, ESA SP-672, 7, 2009.
[38] B. Carry, et al., Potential asteroid discoveries by the ESA Gaia mission: Results from follow-up observations, Astronomy and Astrophysics, 648, A96, 2021. doi: 10.1051/0004-6361/202039579.
[39] The Minor Planet Center (MPC) of the International Astronomical Union. URL: https://minorplanetcenter.net.
[40] List of Observatory Codes: IAU Minor Planet Center. URL: https://minorplanetcenter.net/iau/lists/ObsCodesF.html
[41] G. Adam, et al., Embedded microcontroller with a CCD camera as a digital lighting control system, Electronics, vol. 8 (1), pp. 33, 2019. doi: 10.3390/electronics8010033.
[42] S. Khlamov, et al., Development of computational method for matched filtration with analytic profile of the blurred digital image, Eastern-European Journal of Enterprise Technologies, vol. 5, issue 4-119, pp. 24–32, 20222. doi: 10.15587/1729-4061.2022.265309.
[43] O. Ilbert, et al., Accurate photometric redshifts for the CFHT legacy survey calibrated using the VIMOS VLT deep survey, Astronomy & Astrophysics, vol. 457 (3), pp. 841-856, 2006. doi: 10.1051/0004-6361:20065138.
[44] N. M. Ball, and R. J. Brunner, Data mining and machine learning in astronomy, International Journal of Modern Physics D, vol. 19 (7), pp. 1049–1106, 2010. doi: 10.1142/S0218271810017160.
[45] L. Kirichenko, A.S.A. Alghawli, T. Radivilova, Generalized approach to analysis of multifractal properties from short time series, International Journal of Advanced Computer Science and Applications, vol. 11, issue 5, pp. 183–198, 2020. doi: 10.14569/IJACSA.2020.0110527.